

Temporal measurement of hot-electron relaxation in a phonon-cooled metal island

D. R. Schmidt, C. S. Yung, and A. N. Cleland*

Department of Physics and iQUEST, University of California at Santa Barbara, Santa Barbara, California 93106, USA

(Received 25 February 2004; published 23 April 2004)

We report temporal measurements of the dynamic electronic temperature and the electron-phonon thermal relaxation rate in a micron-scale metal island, with an electronic heat capacity of order 1 fJ/K ($C \sim 10^7 k_B$). We employed a superconductor–insulator–normal-metal tunnel junction, embedded in a radio-frequency resonator, as a fast (~ 20 MHz) thermometer. A resistive heater coupled to the island allowed us to pulse the electronic temperature well above the phonon temperature. Using this device, we have determined the thermal relaxation rate of a hot-electron population in a thin normal-metal film with a measurement bandwidth that exceeds the low-temperature thermal bandwidth.

DOI: 10.1103/PhysRevB.69.140301

PACS number(s): 63.20.Kr, 65.40.Ba, 65.90.+i

Determination of the heat capacity C of a thermodynamic system, in contact with a thermal reservoir through a thermal conductance G , necessitates the measurement of temperature over time scales shorter than the characteristic thermal relaxation time $\tau = C/G$. For mesoscopic devices, this time scale can become exceedingly short. A contributing factor is that both the electron and phonon heat capacities scale with device volume V . Furthermore, it is difficult to thermally isolate a phonon system from its environment, as even a very weak mechanical suspension can be limited at low temperatures by the scale-independent quantum of phonon thermal conductance.^{1–4} Electrons in a metal, however, naturally decouple from their phonon environment at low temperatures, with the electron-phonon thermal conductance scaling with a power law $G_{e-p} \propto VT^{1+m}$. Since the electron heat capacity of a metal scales as $C_e \propto VT$, the small signal electron-phonon thermal relaxation time $\tau_{e-p} = C_e/G_{e-p}$ is independent of volume and scales with a power law T^{-m} . As the exponent m typically is greater than unity, τ_{e-p} increases with decreasing temperature, becoming the dominant relaxation time constant for electrons at low temperatures. Measurements of the electron-phonon coupling to date have relied on static methods,^{5,6} with the detailed temperature dependence and thus the value of m depending upon the sample characteristics.^{7–10}

In an effort to both explicitly measure τ_{e-p} and perform calorimetry at the smallest size scale, we present large-bandwidth measurements of the dynamic electron temperature of a micron-scale metal island, using our recently developed radio-frequency superconductor–insulator–normal-metal thermometer (rf-SIN).¹¹ Static heating measurements can only implicitly access τ_{e-p} , typically by measuring G_{e-p} and assuming the usual linear temperature dependence for the electronic heat capacity. Our measurement has sufficient bandwidth with which to directly measure the relaxation rate at temperatures up to 1 K, and represents the time-domain measurement of τ_{e-p} in a thin normal-metal film. This system therefore allows us to probe the thermodynamic behavior of electrons in very small metal volumes, potentially with heat capacities as small as $10k_B$. Such small metal volumes are prime candidates for energy absorbers in far-infrared photon-counting bolometers,³ and would allow unprecedented calorimetric sensitivity in the mesoscopic regime. Measurements

over time scales shorter than τ_{e-p} are also critical for developing a complete understanding of the thermodynamics of mesoscopic systems.

A commonly accepted model of the thermal decoupling of electrons and phonons at low temperatures was first described theoretically by Little,¹² with a more general discussion provided by Gantmakher.¹³ For bulk metals with volume V , the power flow P_{e-p} from the electron gas at temperature T_e to the phonon gas at T_p is given by

$$P_{e-p} = \Sigma V (T_e^n - T_p^n), \quad (1)$$

where Σ is a material-dependent parameter. For a spherical Fermi surface and a Debye phonon gas, it has been calculated that $n = 5$. From Eq. (1) and a specific-heat scaling as T , we get $\tau_{e-p} \propto T^{-m}$, with $m = n - 2 = 3$.

A number of measurements have shown that Eq. (1) applies to the *static* heating of thin-film metals, typically with n slightly lower than 5, falling in the range from 4.5 to 4.9, with values for Σ in the range $(1-2) \times 10^9$ W/m³ K⁵ (Refs. 3, 5, 6, and 14). Static measurements⁷ of other materials as well as theoretical calculations^{9,10} support $m \approx 2$, while others⁸ indicate $m \approx 4$. The specific temperature dependence of τ_{e-p} thus reflects the properties of the metal, making direct measurements of τ_{e-p} highly relevant.

Our measurements yield the dynamic temperature response of a small metal island by using a SIN tunnel junction thermometer.^{3,14} Well below the superconducting transition temperature T_C , the tunnel junction's small-signal resistance at zero bias, $R_0 \equiv dV/dI(0)$, is exponentially dependent on the ratio of temperature T to the superconducting energy gap Δ , $R_0 \propto e^{\Delta/k_B T}$. A submicron scale SIN tunnel junction therefore has a low-temperature resistance that can easily exceed $10^4 \Omega$, limiting conventional time-domain measurements to bandwidths of order 1 kHz. In order to monitor changes in this resistance at sub-microsecond time scales, we circumvent the unavoidable stray capacitance in the measurement circuit by embedding the junction in a LC resonant circuit, as shown in Fig. 1.^{11,15} We then measure the resistance of the SIN junction, and thus the normal-metal electron temperature, by measuring the power reflected from the circuit at the LC resonance frequency. A change of the junction resistance R_0 , induced by heating the electrons, in turn changes the

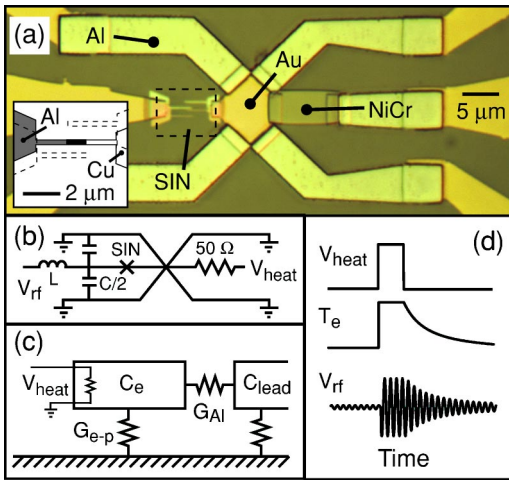


FIG. 1. (Color online) (a) Optical micrograph of electron calorimeter. Center Au island is contacted on left by rf-SIN thermometer, and on right by a NiCr resistor. Outer ground leads and the contact right of the resistor are superconducting Al. Inset: Drawing of the SIN junction: Al gray, Cu white, junction area in black. Dotted outlines are fabrication artifacts. (b) Electrical circuit. SIN thermometer is in a LC resonator. (c) Thermal schematic. Calorimeter electron gas C_e is thermally isolated by superconducting Al contacts (G_{Al}); the dominant thermal link is through G_{e-p} . The NiCr resistor directly heats the electron gas. (d) Timing diagram. The heater voltage pulse causes T_e to rise, saturate, and then decay. The envelope of the reflected power from the LC resonator is directly related to T_e .

amplitude of the reflected radio-frequency signal. This rf-SIN readout scheme is analogous to that employed in the radio-frequency single electron transistor (rf-SET).¹⁶

Our device is fabricated on a single-crystal GaAs chip. A 85 nm thick Au center island, wire-bond pads, and an intermediate Au pad were deposited first. We then deposited a 100 nm thick NiCr film, with a 50Ω resistance, followed by the superconducting Al ground leads and heater contact.¹⁷ The NiCr contacts the Al *via* the intermediate Au pad to ensure low interfacial resistivity. The tunnel junction thermometer was deposited last, using a standard double-angle evaporation method:¹⁸ A 90 nm thick Al electrode was evaporated, oxidized, and the junction completed with a 90 nm thick Cu counterelectrode, which also contacted the center Au island.

The device is shown in Fig. 1(a). Note that the Au center island is electrically grounded, so that heating signals applied to the NiCr resistor do not couple directly to the SIN junction, but instead affect it by changing the temperature of the Au island. The heating signals are in principle limited by the diffusion time from the NiCr through the Au island, and then along the Cu electrode to the tunnel junction; we estimate this time to be less than 10 ns.

We mounted the chip on a printed circuit board, which was enclosed in a brass box. Gold wire bonds were made between the Au bond pads on the chip and Cu coplanar striplines on the circuit board. A chip inductor with $L = 390$ nH was placed in series with the SIN junction. The capacitance C in parallel with the junction is due to the stray geometric

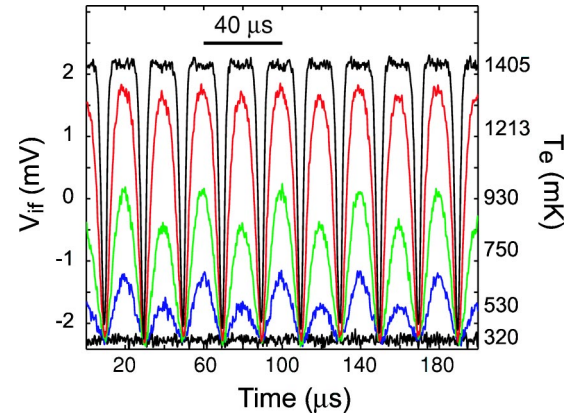


FIG. 2. (Color online) Response to a 25 kHz heater drive (*left axis*: mixer if voltage, *right axis*: electron temperature). Thermometer response is at 50 kHz. Each trace represents 256 averages with a 2 MHz low-pass filter. Baseline signal is for zero heater power, with power ranging from 300 pW to 100 nW. At the highest power the signal clips at $T = T_C \approx 1400$ mK. The 25 kHz components at low power are due to a dc offset in the heater signal.

capacitance of the stripline and Au bond pads, with $C = 0.5$ pF. The expected LC resonance frequency is $f_{res} = 1/2\pi(LC)^{1/2} \approx 350$ MHz, the tuned circuit quality factor is $Q = \sqrt{L/CZ_0^2} \approx 20$, and the measurement bandwidth is $\Delta f = f_{res}/Q \approx 20$ MHz. The measurement circuit is shown in Fig. 1(b). The tunnel junction is configured for simultaneous dc and rf measurements *via* a bias tee, not shown in Fig. 1.

We have described the technical aspects of rf-SIN thermometry elsewhere.¹¹ Here we will describe the salient aspects as they pertain to these measurements. We determined the resonance frequency of the LC circuit to be 345 MHz. A carrier signal source was connected through a directional coupler to a coaxial line, which was in turn connected to the LC resonant circuit. The carrier frequency was set close to the LC resonant frequency.¹⁹ The signal reflected from the LC resonator was high-pass filtered and amplified. This amplified signal was then mixed with a local oscillator (lo), provided by a second rf signal source phase locked to the carrier source. The intermediate frequency (if) output from the mixer was low-pass filtered, amplified, and the resulting time-dependent signal captured by a sampling oscilloscope. The NiCr resistor was heated using either a dc or a rf pulsed source: A pulse sent to the resistor heats the NiCr, the Au island, and the Cu electrode, changing the electron temperature, and therefore changing the amplitude of the carrier signal reflected from the tuned LC circuit, as shown in Fig. 1(d).

In order to characterize the response of the system, we first heated the NiCr resistor using a $f_0 = 25$ kHz sinusoidal drive signal. Figure 2 shows the response for various drive powers. The if signal was low-pass filtered ($f < 2$ MHz), and each curve is the result of averaging 256 drive periods. The left axis is the mixer if voltage, and the labels on the right axis indicate the electron temperature inferred from the change in reflected signal. The instantaneous power dissipated in the resistor is proportional to the square of the voltage applied the heater [$P(t) = V^2(t)/R_{NiCr}$]; this causes the

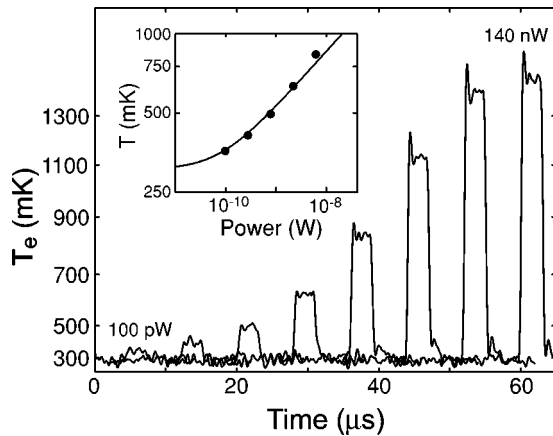


FIG. 3. Composite response to pulsed heating signals, with $3.0 \mu\text{s}$ pulses with peak power 0.1, 0.3, 0.8, 2.2, 6.2, 17.6, 49.0, and 140 nW. The electron temperature is used to determine $P(T_e, T_p)$. Inset: Solid line is fit to $P(T_e, T_p) = V \Sigma (T_e^n - T_p^n)$.

reflected signal to be modulated at twice the heater signal, $2f_0 = 50 \text{ kHz}$. At low powers P , contributions at 25 kHz were also present due to a small dc offset on the heater voltage $V(t)$, $V(t) = V_{dc} + V_0 \sin 2\pi f_0 t$. At the highest powers, the reflected signal is clipped near the Al superconducting transition temperature: The junction resistance is temperature independent above T_C .

The measured signal depends on the proper adjustment of the detection mixer's lo phase. In order to correctly adjust this phase, we first applied a heater signal sufficient to get the maximum (clipped) response, achieved for an island temperature reaching the T_C of the aluminum superconductor of 1.4 K. The phase of the lo was then adjusted to achieve maximum differential response between the lowest ($\cong 300 \text{ mK}$) and the highest ($\cong 1400 \text{ mK}$) electron temperatures. The SIN junction ranges from 105 k Ω to 6 k Ω over this temperature range, and passes through the value of R_0 where optimal matching with the cable impedance occurs.²⁰ In the parlance of radio-frequency electronics, the carrier signal is overmodulated, so the absolute value of the reflected power is a double-valued function of temperature. However, as we are sensitive to the phase of the carrier, the proper quadrature of the mixer if voltage retains a monotonic response. Finally, the reflected if signal as a function of cryostat temperature, for no heater voltage applied, was used to construct the temperature calibration, $V_{if}(T)$.

We measured the *quasistatic* relation between the electron-phonon power flow P_{e-p} and the electron and phonon temperatures T_e and T_p , as given by Eq. (1). We applied a series of $3 \mu\text{s}$ pulses while varying the peak heating power, and monitored the resulting time-dependent electron temperature. The substrate temperature was kept at 300 mK. The signal was filtered with a 2 MHz low-pass filter, and the result of 256 averages is shown in Fig. 3. This is equivalent to a dc heating measurement with a key difference, namely, that as the heating pulses were delivered to the device at a 1 kHz repetition rate, the duty cycle was only 0.3%, so that the substrate phonons did not have sufficient time to heat. The corresponding dc experiment requires 300 times as much

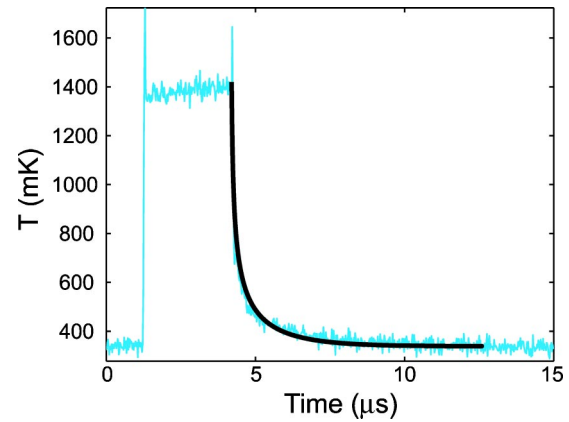


FIG. 4. (Color online) Response to 140 nW, $3.0 \mu\text{s}$ pulse. Solid line is a fit, as discussed in text. Spikes at pulse start and end are due to ringing in the amplifier circuit.

power, with significant phonon heating and a distorted temperature dependence a likely outcome. We find a fitted relation matching that of Eq. (1), with $n=4.7$ and $\Sigma = 2.1 \times 10^9 \text{ W/m}^3 \text{ K}^{4.7}$, consistent with other measurements in the dirty limit.^{3,5,6,14}

Finally, we performed measurements of *dynamic* electron-phonon cooling, by monitoring the detailed time-dependent behavior of the electron temperature at the end of a heating pulse. Figure 4 shows the measured response to a heater pulse (2560 averages, using a 50 MHz low-pass filter). The heating voltage pulse was configured to have 1.6 ns leading and trailing edge widths. The initial temperature rise is at least as fast as the time resolution of the measurement, with an expected rate $\dot{T} = P/C_e \cong 140 \text{ mK/nsec}$, as we are directly heating the electron population. The rapid onset also indicates that electron diffusion in the composite metal structure is not a rate-limiting factor. At the end of the pulse, the heating power drops to zero, leaving a nonequilibrium hot-electron population that relaxes by phonon emission. Initially this relaxation is seen to be quite rapid, but it slows markedly as the electron temperature nears the phonon temperature. The asymmetry of the response shape reflects the temperature dependence of the electron-phonon time constant and the nondifferential nature of the heat pulse; at high temperatures τ_{e-p} is very short, while as the gas cools the time constant becomes significantly larger.

The shape of the relaxation curve shown in Fig. 4 can be understood by examining the dynamics of the electron temperature. The electron heat capacity is $C_e = \gamma V T_e$, where γ is the Sommerfeld constant. Assuming the power flow to the phonons is given by Eq. (1), the time rate of change of the electron temperature \dot{T}_e is

$$\dot{T}_e = - \frac{\Sigma}{\gamma} \left(T_e^{n-1} - \frac{T_p^n}{T_e} \right). \quad (2)$$

Using the normalized temperature $\theta \equiv T_e/T_p$, this is

$$\dot{\theta} = - \frac{1}{n} \frac{1}{\tau_{e-p}(T_p)} (\theta^{n-1} - 1/\theta), \quad (3)$$

in terms of the small signal thermal relaxation rate $\tau_{e-p}^{-1} = n \Sigma T_p^{n-2} / \gamma$ for electrons near the phonon temperature.²¹ We fit our measured response to Eq. (3) using this rate as the only adjustable parameter, finding the value $\tau_{e-p} = 1.6 \mu\text{s}$ at $T_p \cong 300 \text{ mK}$.²² This is in agreement with the measured value of Σ and a composite γ which takes into account the relative metal volumes in the device.²³ We can thus determine the heat capacity of the metal island, $C_e \sim 1 \text{ fJ/K} \cong 10^7 k_B$ at 300 mK. Our explicit measurement finds $\tau_{e-p} \propto T^m$ with $m \approx -3$, consistent with static measurements on similar material systems.^{3,5,6}

There are interesting opportunities for electronic calorimetry in this temperature and size regime. Intriguing theoretical results have been presented for the thermodynamic response of mesoscopic superconducting disks,²⁴ and giant moment electronic paramagnets such as PdMn (Ref. 25) and PdFe (Ref. 26) offer a means of probing the thermodynamics of a mesoscopic phonon-electron-spin-coupled system.

We can estimate the potential calorimetric limits of our technique. Using a cryogenic front end amplifier to measure the reflected power from the SIN junction, we project that a temperature sensitivity of $\approx 1 \mu\text{K/Hz}^{1/2}$ (Ref. 11) is achievable with normal-metal volumes of $0.01\text{--}0.1 \mu\text{m}^3$ that have

heat capacities of $\sim (10^4\text{--}10^5)k_B$ at 300 mK. We estimate that a calorimeter based on a steady-state ac measurement²⁷ will then have a sensitivity of $(50\text{--}500)k_B/\text{Hz}^{1/2}$. Calorimetry at the single degree of freedom scale is accessible with reasonable integration times.

In summary, we have performed sub-microsecond time scale measurements of the electron temperature of a micron scale metal island, cooled dynamically by phonon emission. The ability to apply and measure the response to fast heat pulses has permitted us to make measurements of electron-phonon thermal relaxation in a thin normal-metal film, and extract the heat capacity of the metal island. This, to our knowledge, is the smallest measured heat capacity to date. The device that we have fabricated is a major step forward for mesoscopic thermodynamics, provides a platform for sub-aJ/K calorimetry, and can potentially play an important role in future single photon and phonon bolometers.

We acknowledge financial support provided by the NASA Office of Space Science under Grants Nos. NAG5-8669 and NAG5-11426, the Army Research Office under Grant No. DAAD-19-99-1-0226, and the Center for Nanoscience Innovation for Defense. We thank Bob Hill for processing support.

*Electronic address: cleland@physics.ucsb.edu

¹L.G.C. Rego and G. Kirczenow, Phys. Rev. Lett. **81**, 232 (1998).

²K. Schwab, E.A. Henriksen, J.M. Worlock, and M.L. Roukes, Nature (London) **404**, 974 (2000).

³C.S. Yung, D.R. Schmidt, and A.N. Cleland, Appl. Phys. Lett. **81**, 31 (2002).

⁴A.N. Cleland, D.R. Schmidt, and C.S. Yung, Phys. Rev. B **64**, 172301 (2001).

⁵M.L. Roukes, M.R. Freeman, R.S. Germain, R.C. Richardson, and M.B. Ketchen, Phys. Rev. Lett. **55**, 422 (1985).

⁶F.C. Wellstood, C. Urbina, and J. Clarke, Phys. Rev. B **49**, 5942 (1994).

⁷J.F. DiTusa, K. Lin, M. Kubota, M. Park, M.S. Isaacson, and J.M. Parpia, Phys. Rev. Lett. **68**, 1156 (1992).

⁸M.E. Gershenson, D. Gong, T. Sato, B.S. Karasik, and A.V. Sergeev, Appl. Phys. Lett. **79**, 2049 (2001).

⁹J. Rammer and A. Schmid, Phys. Rev. B **34**, 1352 (1986).

¹⁰D. Belitz and S. Das Sarma, Phys. Rev. B **36**, 7701 (1987).

¹¹D.R. Schmidt, C.S. Yung, and A.N. Cleland, Appl. Phys. Lett. **83**, 1002 (2003).

¹²W.A. Little, Can. J. Phys. **37**, 334 (1959).

¹³V.F. Gantmakher, Rep. Prog. Phys. **37**, 317 (1974).

¹⁴M. Nahum and J.M. Martinis, Appl. Phys. Lett. **63**, 3075 (1993).

¹⁵The intrinsic electrical bandwidth is $f_{3 \text{ dB}} = 1/2 \pi R_0 C_J$, with tunnel resistance R_0 and junction capacitance C_J . For a fixed tunnel barrier thickness, this is independent of junction area A . With typical values of $R_0 A \sim 10^3 \Omega \mu\text{m}^2$ and $C_J/A \sim 10^{-13} \text{ F}/\mu\text{m}^2$, this corresponds to $f_{3 \text{ dB}} \sim 2 \text{ GHz}$.

¹⁶R.J. Schoelkopf, P. Wahlgren, A.A. Kozhevnikov, P. Delsing, and D.E. Prober, Science **280**, 1238 (1998).

¹⁷The thermal conductance of the Al ground leads is given by the Wiedemann-Franz relation, exponentially suppressed by superconductivity, $G_{Al} \approx L_0 T / R_{Al} \exp[-\Delta(T)/k_B T]$, where L_0 is the Lorentz constant and R_{Al} the combined normal-state resistance of the leads ($\approx 0.25 \Omega$), with G_{e-p} given by the derivative of Eq. (1). We estimate G_{e-p}/G_{Al} to be 3, 10, and 120 at $T = 1.4 \text{ K}$, 1.0 K , and 0.3 K , respectively. The SIN junction resistance is always greater than $1 \text{ k}\Omega$ and has a negligible contribution to the thermal conductance.

¹⁸T.A. Fulton and G.J. Dolan, Phys. Rev. Lett. **59**, 109 (1987).

¹⁹Typically -100 dB (100 fW), the rf-SET of Ref. 16 can tolerate much higher power than the rf-SIN.

²⁰The calculated value is at $R_0 = L/CZ_0 \sim 11 \text{ k}\Omega$.

²¹To recover the small signal response for $n=5$, rewrite Eq. (2) in terms of the reduced temperature $\epsilon \equiv (T_e - T_p)/T_p = \theta - 1$ and retain terms $O(\epsilon)$, $\dot{\epsilon} = 5(\Sigma/\gamma)T_p^{n-2}\epsilon$.

²²For simplicity, we used $n=5$ for the fit.

²³The volumetric fractions of Cu, Au, and NiCr in our device are 5%, 65%, and 30%, respectively. Based on bulk data, we estimate the fractional contributions to the heat capacity are 1%, 14%, and 85%. For references to heat capacity measurements see: O.V. Lounasmaa, *Experimental Principles and Methods Below 1 K* (Academic, London, 1974).

²⁴P.S. Deo, J.P. Pekola, and M. Manninen, Europhys. Lett. **50**, 649 (2000).

²⁵G.J. Nieuwenhuys, Adv. Phys. **24**, 515 (1975).

²⁶R.P. Peters, C. Buchal, M. Kubota, R.M. Mueller, and F. Pobell, Phys. Rev. Lett. **53**, 1108 (1984).

²⁷P.F. Sullivan and G. Seidel, Phys. Rev. **173**, 679 (1968).